Proc. Natl. Acad. Sci. USA
Vol. 75, No. 12, pp. 5746–5750, December 1978
Chemistry

Fluorescence energy transfer in the rapid-diffusion limit

(Förster transfer/spectroscopic rulers/terbium/membrane vesicles)

DAVID D. THOMAS, WILLIAM F. CARLSEN, AND LUBERT STRYER

Department of Structural Biology, Sherman Fairchild Center, Stanford University School of Medicine, Stanford, California 94305

Communicated by John I. Brauman, August 18, 1978

ABSTRACT **Energy transfer is enhanced by translational diffusion of the donor and acceptor [Steinberg, I. Z. & Katchalski, E. (1968) *J. Chem. Phys.* 48, 2404–2410]. The effect of diffusion on energy transfer depends on $D\tau_0/s^2$, in which D is the sum of the diffusion coefficients of the donor and acceptor, τ_0 is the lifetime of the donor in the absence of transfer, and s is the mean distance between donors and acceptors. In most previous studies, $D\tau_0/s^2 \ll 1$, corresponding to the static limit. We report here steady-state and kinetic fluorescence experiments showing that $D\tau_0/s^2 \gg 1$, the rapid-diffusion limit, can be attained by using Tb^{3+} chelated to dipicolinate as a long-lived energy donor (τ_0 = 2.2 msec). The concentration of rhodamine B, the energy acceptor, resulting in 50% transfer was 0.67 μM, which is three orders of magnitude less than the concentration giving 50% transfer in the static limit. The dependence of the transfer efficiency on diffusion coefficients varying from 5×10^{-11} to 1.5×10^{-4} cm²/sec, spanning the range from the static limit to the rapid-diffusion limit, is in excellent agreement with theory. It is evident that energy donors with millisecond or longer excited state lifetimes can be used to probe translational motions in membranes and other assemblies. Energy transfer in the rapid diffusion limit is sensitive to the distance of closest approach (a) of the donor and acceptor. For a Tb·(DPA)$_3$ chelate trapped inside the aqueous space of a membrane vesicle containing eosin phosphatidylethanolamine, a = 10 Å. The transverse location of chromophores in model membranes and biological membranes can be determined by this technique.**

Fluorescence energy transfer has often been used to measure distances between stationary donors and acceptors (1–4). If diffusion substantially changes the distances between donors and acceptors during the excited state lifetime of the donor, energy transfer can be enhanced, as shown theoretically by Steinberg and Katchalski (5) and verified experimentally by Elkana *et al.* (6). Haas *et al.* (7) have recently determined the diffusion coefficients of the ends of oligopeptide chains in solution by analyzing the effect of diffusion on energy transfer. In the present study, we consider the limiting case in which energy transfer is maximally enhanced by diffusion—i.e., a further increase in the diffusion coefficient has no further effect on the transfer efficiency. Our theoretical analysis of this rapid-diffusion limit shows that these experiments are sensitive to the distance of closest approach between donor and acceptor and that measurements are possible at much lower acceptor concentrations than in the absence of diffusion (the static limit). Calculations using the theory of Steinberg and Katchalski (5) show that, for small molecules in aqueous solution, the rapid-diffusion limit cannot be reached with conventional fluorescent donors having excited state lifetimes in the nanosecond range. This limit can be attained only if the fluorescent donor has a much longer lifetime, in which extensive diffusion can occur.

In order to attain the rapid-diffusion limit and test the theory, we have used as a donor the fluorescent lanthanide ion Tb^{3+}, which has a lifetime in the millisecond range (8, 9). Tb^{3+} was chelated to dipicolinic acid (DPA), resulting in a fluorescence enhancement of about 10^4 (10). This Tb·(DPA)$_3$ chelate consists of three molecules of DPA liganded to Tb^{3+} and has a net charge of −3 above pH 5 (10). Experiments using Tb·(DPA)$_3$ as the donor and either rhodamine B or nitrobenzodioxazole (NBD) diethanolamine as the acceptor verify the validity of the theory over the entire range from the static limit to the rapid-diffusion limit and demonstrate that the rapid-diffusion limit has been reached for these molecules in aqueous solution at room temperature.

We have also used energy transfer in the rapid-diffusion limit to measure the distance from the aqueous surface to an acceptor chromophore in a membrane. We present a theoretical analysis and report experiments on energy transfer from Tb·(DPA)$_3$, trapped in the inner aqueous space of phospholipid vesicles, to acceptors in the membrane. The results indicate that this is a promising technique for measuring the transverse location of chromophores in biological membranes.

THEORY

In Förster's theory of dipole–dipole energy transfer (1), the rate constant k_T for energy transfer is

$$k_T = k_0(r/R_0)^{-6} \quad [1]$$

in which k_0 is the sum of the rate constants for the decay of the excited donor in the absence of acceptor and r is the distance between the donor and acceptor. R_0, the distance in Å at which the transfer efficiency is 50% for a single donor–acceptor pair, is given by

$$R_0 = (JK^2Q_0n^{-4})^{1/6} \times 9.79 \times 10^3 \quad [2]$$

in which J is the spectral overlap integral (in cm³ M⁻¹), K^2 is the orientation factor, Q_0 is the quantum yield of the donor in the absence of transfer, and n is the refractive index of the medium. The rate of decay of the excited donors is

$$\frac{dn^*}{dt} = -(k_0 + k_T)n^* \quad [3]$$

in which n^* is the number of excited donors. The efficiency of energy transfer E is

$$E = k_T/(k_T + k_0). \quad [4]$$

Experimentally, E is determined from the ratio of the quantum yield Q in the presence of acceptor to that in its absence,

$$E = 1 - Q/Q_0, \quad [5]$$

or from the corresponding ratio of excited state lifetimes,

$$E = 1 - \tau/\tau_0 \quad [6]$$

in which $\tau = (k_0 + k_T)^{-1}$ is the lifetime of the donor in the

The publication costs of this article were defrayed in part by page charge payment. This article must therefore be hereby marked "*advertisement*" in accordance with 18 U. S. C. §1734 solely to indicate this fact.

Abbreviations: DPA, dipicolinic acid; Tb·(DPA)$_3$, chelate consisting of one terbium ion (Tb^{3+}) and three dipicolinate ions (DPA^{2-}); NBD, nitrobenzodioxazole.

presence of acceptor and $\tau_0 = k_0^{-1}$ is the lifetime in the absence of acceptor.

In an ensemble of stationary donors and acceptors, the decay rate for a single donor is a sum of k_T terms (Eq. 1) over the acceptors. Only those donors having at least one acceptor within a distance comparable to R_0 will have an appreciable probability of energy transfer. By contrast, in the presence of translational diffusion, energy transfer is no longer restricted to donors that have an acceptor within this distance at the instant of excitation. Transfer will additionally occur between donors and acceptors that come within a distance of about R_0 during the donor's lifetime. Specifically, the mean distance diffused by the donor and acceptor relative to each other during τ_0 must be comparable to s, the mean intermolecular distance, for diffusion to enhance energy transfer. Because the mean square distance diffused in a time t is $6Dt$ (in three dimensions), in which D is the diffusion coefficient, diffusion will substantially increase energy transfer if $6D\tau_0 \geq s^2$.

The effect of diffusion on energy transfer has been analyzed theoretically by Steinberg and Katchalski (5). They derived a partial differential equation for the kinetics of energy transfer (equation 33 in ref. 5), which contains a diffusion term that changes the distance between donors and acceptors during the lifetime of the excited donor. The transfer efficiency calculated by solving this equation numerically (6, 11, 12) depends on R_0, a, and the concentration of acceptor, as in the absence of diffusion. In addition, the transfer efficiency depends on the product of D and τ_0. The results of these calculations for $R_0 =$ 50 Å, $a = 5$ Å (a plausible value for the closest approach of two small molecules in solution), and an acceptor concentration of 0.1 mM are shown in Fig. 1, which depicts the dependence of the transfer efficiency on D for $\tau_0 = 1$ nsec, 1 μsec, 1 msec, and 1 sec. The curve for $\tau_0 = 1$ msec is shown over the entire range of its variation. For $D < 10^{-10}$ cm^2/sec, E approaches a constant minimal value. This is the *static limit*, where $D\tau_0/s^2 \ll 1$. For D between about 10^{-10} and 10^{-6} cm^2/sec, E is sensitive to diffusion. This is the intermediate range, where $6D\tau_0/s^2 \approx 1$. For D > 10^{-6} cm^2/sec, E approaches a constant maximal value. This is the *rapid-diffusion limit*, where $D\tau_0/s^2 \gg 1$. Because E is a function of the product of D and τ_0, the other curves in Fig. 1 are simply shifted to the right or left. The curve for $\tau_0 = 1$ nsec emphasizes that energy donors having this lifetime are insensitive to diffusion, because even the smallest molecules have diffusion coefficients of 10^{-5} cm^2/sec or less in water at 20°C. The enhancement of energy transfer by diffusion becomes significant when τ_0 is 1 μsec or longer for donor–acceptor pairs having $D < 10^{-6}$ cm^2/sec. Because even small molecules in aqueous solution have diffusion coefficients less than 10^{-5} cm^2/sec, it is evident from Fig. 1 that the rapid-diffusion limit for typical donor–acceptor pairs can only be attained by using donors with $\tau_0 \geq 1$ msec. Accordingly, we have chosen the fluorescent lanthanide ion Tb^{3+}, which has a τ_0 of 2.2 msec, to test the validity of this theory.

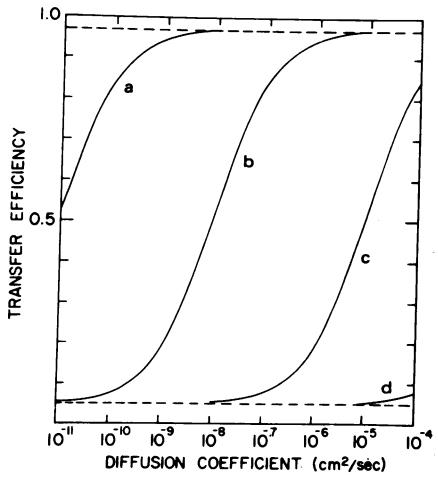

FIG. 1. Effect of diffusion on the efficiency of energy transfer (E) calculated according to equations 11–14 in ref. 5. The abscissa is D, the sum of the diffusion coefficients of the donor and acceptor. In this calculation, $R_0 = 50$ Å, a (distance of closest approach) = 5 Å, and the acceptor concentration is 0.1 mM. The lifetime of the donor in the absence of energy transfer (τ_0) is 1 sec, 1 msec, 1 μsec, and 1 nsec, for the calculated curves a, b, c, and d, respectively. The lower and upper dashed lines denote the transfer efficiencies for the static and rapid-diffusion limits, respectively.

In the static limit, each donor in the ensemble has a different transfer efficiency (E_j). The transfer efficiency E_s of the ensemble is the average over all donors.

$$E_s = \frac{1}{N}\sum_{j=1}^{N} E_j. \quad [7]$$

This limit has been treated in detail by Förster (2). By contrast, all donors of an ensemble are identical in the rapid-diffusion limit. The transfer efficiency E_r for this limit is

$$E_r = k_r/(k_0 + k_r) \quad [8]$$

in which k_r, the sum of the rate constants for transfer from the donor to all acceptors, is

$$k_r = \rho \int\int\int\int k_0 \left(\frac{r}{R_0}\right)^{-6} d^3r \quad [9]$$

$$= \rho \int_a^\infty \frac{1}{\tau_0}\left(\frac{r}{R_0}\right)^{-6} 4\pi r^2 dr \quad [10]$$

$$= 4\pi\rho R_0^6/(3\tau_0 a^3) \quad [11]$$

and ρ is the density of acceptors. An important feature of this equation for the rapid-diffusion limit is the dependence of k_r on a^{-3}, which is illustrated in Fig. 2*A*.

Eq. 9 can be applied to other arrangements of donors and acceptors, provided that the diffusion of one or both is rapid. For example, consider the *inset* in Fig. 2*B*, which depicts a membrane vesicle with a surface density σ of acceptors at radius b and a solution of donors trapped in the inner aqueous volume. The distance of closest approach between these donors and acceptors is a. Integrating Eq. 9 over the internal volume of the vesicle gives

$$k_r = \frac{3\pi\sigma b R_0^6}{2(b-a)^3}\int_0^{b-a} h[(b-h)^{-4} - (b+h)^{-4}]dh. \quad [12]$$

The transfer efficiencies calculated from this equation are plotted in Fig. 2*B*, which shows that the distance of closest approach can be measured over a wide range of values by choosing an appropriate concentration of acceptor.

It should be noted that the above analysis is based on several assumptions. (*i*) The use of a single R_0 value in Eqs. 9–12 is valid if all donor–acceptor pairs have the same value of K^2. In our experiments, this condition is closely approached because the angular dependence is effectively randomized by the combination of rotational and translational diffusions of the donor during its excited state lifetime. (*ii*) The rate of energy transfer due to exchange interactions is assumed to be small compared to that of Förster dipole–dipole energy transfer. This assumption is probably valid for donor–acceptor pairs with R_0 distances of more than about 20 Å. (*iii*) Spherical symmetry is assumed in deriving Eqs. 11 and 12. Eq. 9 can be used as the starting point for treating nonspherically symmetric systems.

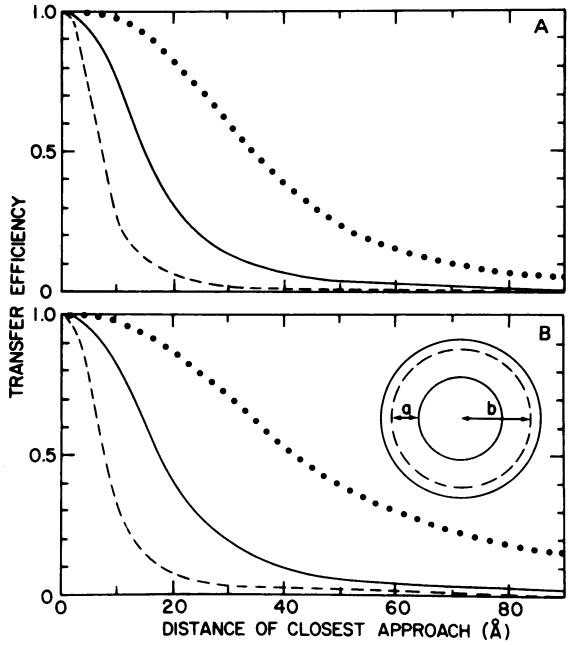

FIG. 2. Effect of the distance of closest approach (a) between the donor and acceptor on the transfer efficiency in the rapid-diffusion limit. R_0 = 50 Å in this calculation. (A) Solution of donors and acceptors. The acceptor concentrations are 1.0 (dotted), 0.1 (solid), and 0.01 (dashed) mM. (B) Solution of donors trapped in the inner aqueous space of a membrane vesicle containing a spherical shell of acceptors at radius b = 150 Å. The surface densities of acceptor are 0.02 (dotted), 0.002 (solid), and 0.0002 (dashed) per phospholipid (acceptors per 70 Å^2).

EXPERIMENTAL METHODS

For time-resolved fluorescence measurements, the excitation source used was a pulsed (cavity-dumped) argon-ion laser (Spectra-Physics 171/365). The 514.5 nm line was focused and then doubled with a temperature phase-matched ADP crystal (Inrad 5-1). The second harmonic (257.25 nm) was separated from the fundamental by a dispersing prism and then filtered (Corning 7-54) to remove stray light. The resulting excitation pulse at the sample was 50 nsec wide, illuminating a 1-mm-diameter spot with $\approx 2 \times 10^8$ photons per pulse. The repetition rates used varied between 20 Hz and 5 kHz, depending on the lifetime of the sample.

The fluorescence emission at right angles was passed through a UV cut-off filter (Corning 0-53) onto a 56AVP photomultiplier (Amperex) biased for single-photon counting. The anode signal was preamplified and discriminated with a single-channel analyzer (Ortec 4890). The resulting pulses were then counted synchronously with the cavity-dump trigger by using a multichannel scaler (Hewlett-Packard 5400).

System timing and amplitude linearity were calibrated with a frequency counter (Hewlett-Packard 5325A) and a random noise source (dark noise of a 56AVP photomultiplier), respectively. The 50-nsec excitation pulse width and the absence of any significant time jitter produced an instrument response function one channel wide, eliminating the need for deconvolution. The photon counting rate was always less than 10^4 Hz, resulting in a scalar dead-time correction of less than 1%. The fluorescence lifetime was determined with a least-squares fit of the data to a single-exponential decay plus a constant background.

Steady-state fluorescence was measured with a photon-counting fluorimeter (Spex Fluorlog). Factors used in correcting emission spectra for the wavelength dependence of the detection system were obtained by using a MgO scatterer normalized against a calibrated photodiode (United Detector PIN 10-UV).

$TbCl_3$ (Alfa), dipicolinic acid (Sigma), and rhodamine B (Eastman) were commercial products. NBD diethanolamine was a gift from Richard Haugland (Molecular Probes, Roseville, MN), and eosin phosphatidylethanolamine was from Bernard Fung. Phosphatidylcholine was prepared from egg yolks (13).

Tb^{3+} was chelated to dipicolinate to enhance its fluorescence by a factor of about 10^4 (10). Solutions containing Tb^{3+} always contained enough DPA to ensure that virtually all of the Tb^{3+} was chelated by DPA. Fluorescent-labeled vesicles containing $Tb\text{-}(DPA)_3$ trapped in their inner aqueous space were prepared by the following procedure (14). Egg phosphatidylcholine and eosin phosphatidylethanolamine were mixed in ethanol solution, at a final phospholipid concentration of 20 mM. A 0.5-ml aliquot of this solution was injected rapidly through a 30-gauge syringe needle into 9.5 ml of a rapidly stirred solution containing 10 mM $TbCl_3$, 50 mM DPA, and 0.1 M Tris, pH 8.0, at 20°C. This vesicle suspension was centrifuged at 80,000 × g for 15 min to remove large liposomes. External $Tb\text{-}(DPA)_3$ was removed by chromatography on Sephadex G-25 (medium).

RESULTS

The emission spectrum of $Tb\text{-}(DPA)_3$, the energy donor, extends from about 470 to 640 nm, overlapping the absorption spectra of the three energy acceptors used in this study (Fig. 3). The spectral overlap integrals (J) are 4.58×10^{-13}, 4.51×10^{-14}, and 5.13×10^{-14} cm^3 M^{-1} for rhodamine B, eosin phosphatidylethanolamine, and NBD diethanolamine, respectively. The R_0 values for transfer to these acceptors are 65.7, 45.6, and 44.6 Å, respectively, assuming $K^2 = 0.67$, $Q_0 = 1$, and $n = 1.33$.

The emission kinetics of $Tb\text{-}(DPA)_3$ in the presence of various concentrations of rhodamine B are shown in Fig. 4. These plots of the logarithm of the fluorescence intensity versus time are linear, indicating that the emission kinetics are characterized by single-exponential decays, as expected for energy transfer in the rapid-diffusion limit. The excited state lifetime decreased from 2.22 msec in the absence of rhodamine B to 0.12 msec in

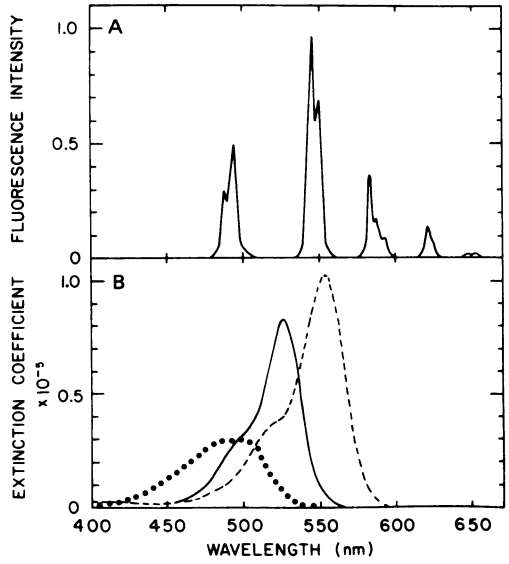

FIG. 3. (A) Fluorescence emission spectrum of $Tb\text{-}(DPA)_3$, the energy donor. The solution contained 10 μM $TbCl_3$/0.1 mM DPA/0.1 M Tris buffer, pH 8, at 20°C. The excitation wavelength was 270 nm. (B) Absorption spectra of the energy acceptors: NBD diethanolamine (dotted), eosin phosphatidylethanolamine (solid), and rhodamine B (dashed). The extinction coefficients are in units of M^{-1} cm^{-1}.

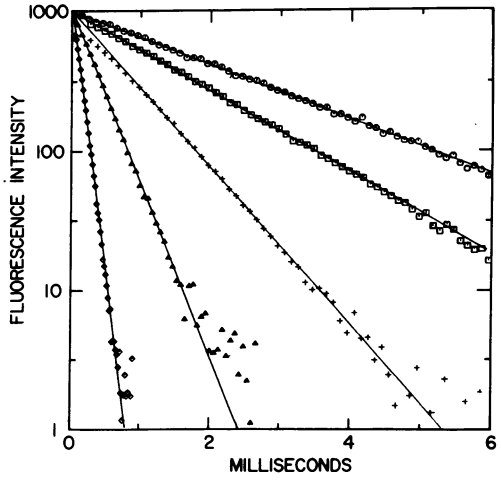

FIG. 4. Dependence of the fluorescence emission kinetics of Tb·(DPA)$_3$, the energy donor, on the concentration of rhodamine B, the energy acceptor. The logarithm of the fluorescence intensity is plotted as a function of time after a 50-nsec exciting light pulse. The solutions contained 10 μM $TbCl_3$/0.1 mM DPA/0.1 M Tris buffer, pH 8, at 20°C. Rhodamine B concentrations of 0 (○), 3×10^{-7} (□), 10^{-6} (+), 3×10^{-6} (△), and 10^{-5} (◇) M gave single-exponential decays of 2.22, 1.49, 0.84, 0.34, and 0.12 msec, respectively.

the presence of 10 μM rhodamine B. Transfer efficiencies calculated from these lifetimes according to Eq. 6 are plotted as a function of the concentration of energy acceptor in Fig. 5. These transfer efficiencies agree closely with those obtained from steady-state fluorescence measurements. Also shown in Fig. 5 are the results of steady-state fluorescence measurements of energy transfer from Tb·(DPA)$_3$ to NBD diethanolamine. The acceptor concentrations resulting in 50% transfer are 0.67 μM for rhodamine B and 7.1 μM for NBD diethanolamine. The dependence of the transfer efficiency on the concentration of these acceptors is in excellent agreement with the curves (solid lines in Fig. 5) calculated according to Eq. 11 for energy transfer in the rapid-diffusion limit, using $R_0 = 65.7$ Å and $a = 5.15$ Å for rhodamine B, and $R_0 = 44.6$ Å and $a = 5.2$ Å for NBD diethanolamine.

The strongest evidence that the rapid-diffusion limit was attained in the preceding experiments comes from a study of

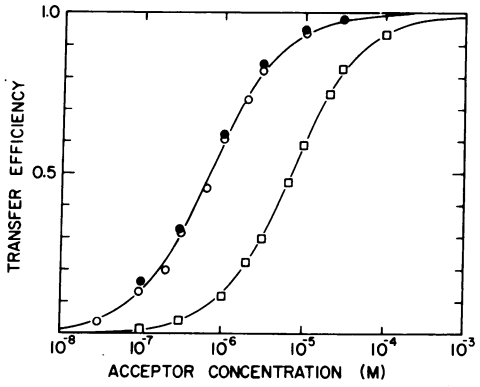

FIG. 5. Effect of the concentration of energy acceptor on the transfer efficiency from Tb·(DPA)$_3$ in the rapid-diffusion limit. Each solution contained 10 μM $TbCl_3$/0.1 mM DPA/0.1 M Tris, pH 8, at 20°C. The acceptors are rhodamine B (○, from steady-state measurements; ●, from lifetime measurements) and NBD diethanolamine (□, from steady-state measurements). Theoretical curves (solid lines) were calculated from Eq. 11, for R_0 values of 65.7 Å for rhodamine B and 44.6 Å for NBD diethanolamine. The distance of closest approach (a) was varied to best fit the experimental points: 5.15 Å for rhodamine B and 5.2 Å for NBD diethanolamine.

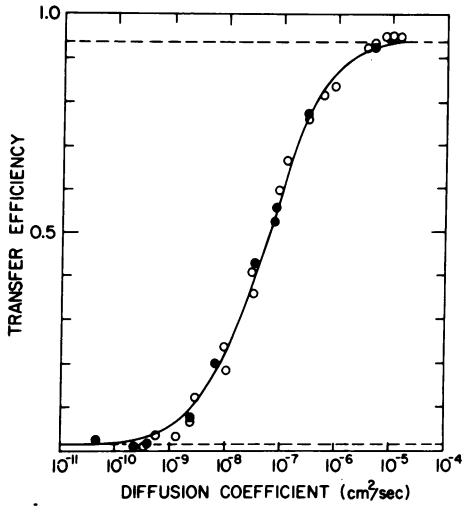

FIG. 6. Effect of diffusion on the efficiency of energy transfer from Tb·(DPA)$_3$ to rhodamine B. The transfer efficiency is plotted as a function of the sum of these diffusion coefficients (D). The solutions contained 10 μM $TbCl_3$/0.1 mM DPA/0.1 M Tris buffer, pH 8, and 10 μM rhodamine B. The solid line is calculated according to equations 11–14 in ref. 5 for $R_0 = 65.7$ Å, $a = 5.15$ Å, acceptor concentration = 10 μM, and $\tau_0 = 2.2$ msec. The observed transfer efficiencies from steady-state fluorescence measurements (○) and from lifetime measurements (●) are shown. The diffusion coefficient was varied by changing the temperature and the concentration of glycerol. The viscosities (η) were then measured and the relative diffusion coefficients were determined by calculating T/η. These diffusion coefficients were placed on an absolute scale by matching the 50% transfer points of the observed and calculated curves.

the dependence of the transfer efficiency on D, the sum of the diffusion coefficients of Tb·(DPA)$_3$ and rhodamine B (Fig. 6). D was varied over seven orders of magnitude by changing the temperature and the concentration of glycerol. The observed transfer efficiencies, ranging from 2 to 94%, are in excellent agreement with the theoretical curve calculated according to equations 11–14 in ref. 5. The diffusion coefficient of 7.6×10^{-6} cm^2/sec in H_2O at 20°C determined in this way is close to the value expected ($6–8 \times 10^{-6}$ cm^2/sec) for these molecules.

Energy transfer in the rapid-diffusion limit was used to de-

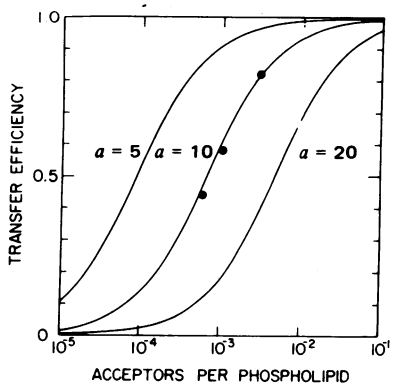

FIG. 7. Effect of the surface density of eosin, the energy acceptor, on the efficiency of energy transfer from Tb·(DPA)$_3$ trapped in the inner aqueous space of membrane vesicles containing eosin phosphatidylethanolamine. The abscissa gives the surface density of energy acceptor, expressed as the number of eosin chromophores per phospholipid, assuming an area of 70 Å^2 per phospholipid. The experimental results for three surface densities of eosin phosphatidylethanolamine are plotted as solid circles. The solid lines were calculated from the theoretical expression in Eq. 7, with $R_0 = 45.6$ Å (determined from the spectra in Fig. 3) and $b = 150$ Å (determined from electron microscopy). The values of a used to calculate these curves are indicated.

termine the distance of closest approach between Tb·(DPA)$_3$ trapped in the inner aqueous volume of a membrane vesicle and the eosin chromophore of eosin phosphatidylcholine incorporated into the bilayer. The transfer efficiencies obtained for 0.0006, 0.0011, and 0.003 acceptors per phospholipid were 44, 58, and 82%, respectively. These observed values are compared with theoretical curves calculated for closest approach distances of 5, 10, and 20 Å in Fig. 7. The best fit is given by a closest approach distance of 10 Å, which is plausible because the acceptor chromophore is attached to the headgroup of the phospholipid.

DISCUSSION

We have attained the rapid-diffusion limit in fluorescence energy transfer by using a long-lived energy donor, Tb^{3+} (τ = 2.2 msec). Eu^{3+} (9) and phosphorescent chromophores such as tryptophan (15) may also be useful in this regard. One of the most striking consequences of the rapid-diffusion limit is that energy transfer occurs at extremely low acceptor concentrations. The transfer efficiency from Tb·(DPA)$_3$ to rhodamine B is 50% at a rhodamine B concentration of 0.67 μM, three orders of magnitude less than the concentration required to achieve the same transfer efficiency in the absence of diffusion. At 0.67 μM, the mean distance between acceptors is approximately 1400 Å. In the static limit, the same transfer efficiency would occur when the mean distance between acceptors is about 130 Å. At such low concentrations, possible perturbations caused by the probes are minimized and inner filter effects are negligible, permitting a more direct and accurate measurement of the transfer efficiency than in the slow-diffusion limit.

Probably the most useful feature of the rapid-diffusion limit is the strong dependence of E on the distance of closest approach, a, between the donor and acceptor. Distances from a few angstroms to greater than R_0 can be determined with precision (Eqs. **11** and **12** and Fig. 2). For example, a solution of long-lifetime donors could be used to measure the distance between the aqueous surface of a protein and an acceptor chromophore in it. This method may be especially valuable in studying membrane proteins. Energy transfer from donors trapped in the inner aqueous space of a membrane vesicle (or alternatively, from donors outside the vesicle) to acceptor chromophores at a fixed distance a from the inside surface provides a direct and sensitive method for the measurement of a (Eq. **12** and Figs. 2*B* and 7). Our preliminary experiments suggest that the retinal chromophore of rhodopsin is closer to the intradisc surface of the disc membrane than to the extradisc surface. The purple membrane and membranes containing cytochrome oxidase are other examples of chromophoric membrane systems that can be studied in this way.

It is interesting to note that electrostatic interactions will alter the distribution of distances between donors and acceptors and thereby change the transfer efficiency. For example, using Tb·(DPA)$_3$ (net charge, −3) as a donor, we have found methylene blue (net charge, +1; R_0, 49 Å) to be a more effective energy acceptor than bromphenol blue (net charge, −1; R_0, 62 Å), a result opposite that predicted from the R_0 values alone. The extent of electrostatic interactions could be ascertained experimentally by varying the ionic strength and by using a series of terbium chelates with different net charges. Alternatively, electrostatic effects can be avoided by using uncharged acceptors, such as rhodamine B and NBD diethanolamine (Fig. 5). The experimentally derived value of 10 Å for the closest approach between Tb·(DPA)$_3$ and eosin phosphatidylethanolamine may be somewhat greater than the actual value because both species are negatively charged.

In addition to making it feasible to attain the rapid-diffusion limit, long-lived donors such as Tb^{3+} permit the measurement of small diffusion coefficients. Calculations of the effect of diffusion on energy transfer in two dimensions show that a donor having a millisecond lifetime can be used to measure diffusion coefficients of 10^{-8} to 10^{-11} cm^2/sec, which are characteristic of proteins in membranes and of membrane lipids in the solid phase.

We thank Dr. Bernard Fung and Dr. Richard Haugland for gifts of fluorescent probes. This work was supported by Research Grants GM-24032 and EY-02005 from the National Institutes of Health. D.D.T. is a Helen Hay Whitney Foundation Postdoctoral Fellow.

1. Förster, T. (1948) *Ann. Physik* **2**, 55–75.
2. Förster, T. (1949) *Z. Naturforsch.* **4a**, 321–327.
3. Stryer, L. & Haugland, R. P. (1967) *Proc. Natl. Acad. Sci. USA* **58**, 719–726.
4. Stryer, L. (1978) *Annu. Rev. Biochem.* **47**, 819–846.
5. Steinberg, I. Z. & Katchalski, E. (1968) *J. Chem. Phys.* **48**, 2404–2410.
6. Elkana, Y., Feitelson, J. & Katchalski, E. (1968) *J. Chem. Phys.* **48**, 2399–2404.
7. Haas, E., Katchalski-Katzir, E. & Steinberg, I. Z. (1978) *Biopolymers* **17**, 11–31.
8. Luk, C. K. (1971) *Biochemistry* **10**, 2838–2843.
9. Horrocks, W. D., Jr., Schmidt, G. F., Sudnick, D. R., Kittrell, C. & Bernheim, R. A. (1977) *J. Am. Chem. Soc.* **99**, 2378–2380.
10. Barela, T. D. & Sherry, A. D. (1976) *Anal. Biochem.* **71**, 351–357.
11. Crank, J. (1975) *The Mathematics of Diffusion* (Clarendon, Oxford), 2nd Ed.
12. Carnahan, B., Luther, H. A. & Willis, J. O. (1969) *Applied Numerical Methods* (Wiley, New York), pp. 440–451.
13. Singleton, W. S., Gray, M. S., Brown, M. L. & White, J. L. (1965) *J. Am. Oil Chem. Soc.* **42**, 53–56.
14. Batzri, S. & Korn, E. D. (1973) *Biochim. Biophys. Acta* **298**, 1015–1019.
15. Saviotti, M. L. & Galley, W. C. (1974) *Proc. Natl. Acad. Sci. USA* **71**, 4154–4158.